Corrections

MEDICAL SCIENCES. For the article "Linkage disequilibrium in human populations," by Christine Lonjou, Weihua Zhang, Andrew Collins, William J. Tapper, Eiram Elahi, Nikolas Maniatis, and Newton E. Morton, which appeared in issue 10, May 13, 2003, of *Proc. Natl. Acad. Sci. USA* (**100,** 6069–6074; First Published April 29, 2003; 10.1073/pnas.1031521100), due to a printer's error, the last three column headings in Table 5 incorrectly contained dashes in "European-Asian," "African-American-Yoruban," and "African-Eurasian" instead of the necessary minus signs. The corrected table appears below.

Table 5. Weighted difference estimates ± standard errors: Samples with cosmopolitan maps

Estimated	Parameter	European − Asian	African-American − Yoruban	African − Eurasian
ε estimated	ε	0.001 ± 0.043	0.162 ± 0.053	0.638 ± 0.046
ε, M estimated	ε	0.005 ± 0.048	0.110 ± 0.052	0.418 ± 0.052
ε, M estimated	$-\ln M$	−0.002 ± 0.006	0.026 ± 0.011	0.130 ± 0.013

www.pnas.org/cgi/doi/10.1073/pnas.1432848100

MEDICAL SCIENCES. For the article "Normal viability and altered pharmacokinetics in mice lacking mdr1-type (drug-transporting) P-glycoproteins," by Alfred H. Schinkel, Ulrich Mayer, Els Wagenaar, Carla A. A. M. Mol, Liesbeth van Deemter, Jaap J. M. Smit, Martin A. van der Valk, Arie C. Voordouw, Hergen Spits, Olaf van Tellingen, J. Mark J. M. Zijlmans, Willem E. Fibbe, and Piet Borst, which appeared in issue 8, April 15, 1997, of *Proc. Natl. Acad. Sci. USA* (**94,** 4028–4033), the authors note the following correction. Fig. 1, and the first few lines of the *Materials and Methods* and *Results* sections, indicate that during gene disruption, exons 3 and 4 of the *Mdr1b* gene were deleted. However, there is an error in the map of the *Mdr1b* gene: exon 3 is positioned upstream (not downstream) of the first indicated *Nco*I site. As a consequence, only exon 4 of *Mdr1b* was deleted, and not exons 3 and 4. For the validity of the *Mdr1b* and *Mdr1a/1b* knockout mouse strains, this error has no consequences: deletion of exon 4 alone still results in a frameshift and still removes the first transmembrane segment plus some flanking sequences in Mdr1b. The absence of Mdr1b at the protein and functional level in the knockout mice also remains well documented. This correction, therefore, does not affect the conclusions of the paper.

www.pnas.org/cgi/doi/10.1073/pnas.1332736100

NEUROSCIENCE. For the article "Transplanted bone marrow generates new neurons in human brains," by Éva Mezey, Sharon Key, Georgia Vogelsang, Ildiko Szalayova, G. David Lange, and Barbara Crain, which appeared in issue 3, February 4, 2003, of *Proc. Natl. Acad. Sci. USA* (**100,** 1364–1369; First Published January 21, 2003; 10.1073/pnas.0336479100), the lettering in the Fig. 2 legend is incorrect. The corrected legend should read: "**Fig. 2.** Neuronal markers colocalize with the Y chromosome. Fluorescent microscopic images of neocortex from patients 2 (*B*, *D*, and *F*) and 3 (*C*) and hippocampus from patients 1 (*A*) and 3 (*E*). The green color represents the immunostaining for neuronal markers Kv2.1 (*A–D*) and NeuN (*E* and *F*), and the red color represents the Y chromosome. All cell nuclei are stained with 4′,6-diamidino-2-phenylindole, a blue fluorescent chromosomal marker. All images are overlays of the images seen through the three separate filters. Arrows point to cells that are labeled with neuronal markers and are also Y chromosome-positive. In the Kv2.1 immunostaining, the initial axons of some neurons can also be visualized. (Scale bars = 10 μm.)"

www.pnas.org/cgi/doi/10.1073/pnas.1332662100

BIOCHEMISTRY. For the article "Crystal structure of a photoactive yellow protein from a sensor histidine kinase: Conformational variability and signal transduction," by Sudarshan Rajagopal and Keith Moffat, which appeared in issue 4, February 18, 2003, of *Proc. Natl. Acad. Sci. USA* (**100,** 1649–1654; First Published January 31, 2003; 10.1073/pnas.0336353100), the authors note that part of Fig. 1*B* was incorrectly labeled as a π helix. It should have been labeled as a 3–10 helix. This correction does not affect the conclusions of the article. The corrected figure and its legend appear below.

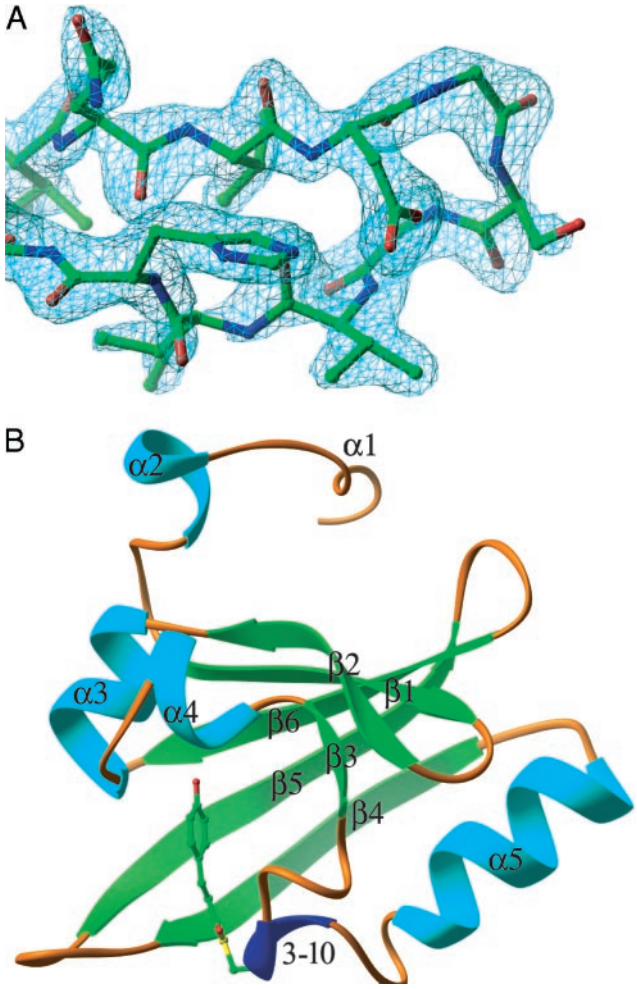

Fig. 1. Crystal structure of Ppr-PYP. (*A*) A simulated annealing composite omit map at 2.0σ level of the β1–β2 turn of chain B. (*B*) Chain B of Ppr-PYP with secondary structure labeled according to ref. 20.

www.pnas.org/cgi/doi/10.1073/pnas.1432896100

Proc. Natl. Acad. Sci. USA
Vol. 94, pp. 4028–4033, April 1997
Medical Sciences

Normal viability and altered pharmacokinetics in mice lacking mdr1-type (drug-transporting) P-glycoproteins

ALFRED H. SCHINKEL*, ULRICH MAYER*, ELS WAGENAAR*, CARLA A. A. M. MOL*, LIESBETH VAN DEEMTER*, JAAP J. M. SMIT*, MARTIN A. VAN DER VALK†, ARIE C. VOORDOUW‡, HERGEN SPITS‡, OLAF VAN TELLINGEN§, J. MARK J. M. ZIJLMANS¶, WILLEM E. FIBBE¶, AND PIET BORST*‖

Divisions of *Molecular Biology, †Molecular Genetics, ‡Immunology, and §Clinical Chemistry, The Netherlands Cancer Institute, Plesmanlaan 121, 1066 CX Amsterdam, The Netherlands; and ¶Department of Hematology, University Medical Center, 2300 RC Leiden, The Netherlands

Contributed by Piet Borst, February 6, 1997

ABSTRACT **The mdr1-type P-glycoproteins (P-gps) confer multidrug resistance to cancer cells by active extrusion of a wide range of drugs from the cell. To study their physiological roles, we have generated mice genetically deficient in the *mdr1b* gene [*mdr1b* (−/−) mice] and in both the *mdr1a* and *mdr1b* genes [*mdr1a/1b* (−/−) mice]. In spite of the host of functions speculatively attributed to the mdr1-type P-gps, we found no physiological abnormalities in either strain. Viability, fertility, and a range of histological, hematological, serum–chemical, and immunological parameters were not abnormal in *mdr1a/1b* (−/−) mice. The high level of mdr1b P-gp normally present in the pregnant uterus did not protect fetuses from a drug (digoxin) in the bloodstream of the mother, although the protein did reduce drug accumulation in the adrenal gland and ovaries. Pharmacologically, *mdr1a/1b* (−/−) mice behaved similarly to the previously analyzed *mdr1a* (−/−) mice, displaying, for instance, increased brain penetration and reduced elimination of digoxin. However, both mdr1a and mdr1b P-gps contributed to the extrusion of rhodamine from hematopoietic progenitor cells, suggesting a potential role for the endogenous mdr1-type P-gps in protection of bone marrow against cytotoxic anticancer drugs. This, and the normal viability of *mdr1a/1b* (−/−) mice, has implications for the use of P-gp-blocking agents in cancer and other chemotherapy. *mdr1a/1b* (−/−) mice should provide a useful model system to further test the pharmacological roles of the drug-transporting P-gps and to analyze the specificity and effectivity of P-gp-blocking drugs.**

The mdr1-type P-glycoproteins (P-gps) are plasma membrane proteins that can cause multidrug resistance in tumor cells by actively extruding an inordinately wide range of structurally diverse, hydrophobic amphipathic compounds from the cell. These compounds include important anti-cancer drugs like anthracyclines, *Vinca* alkaloids, epipodophyllotoxins, and taxanes, and it is likely that P-gp contributes to the (intrinsic or acquired) resistance against chemotherapy occurring in various cancers (for reviews see refs. 1–4).

The discovery of compounds that inhibit P-gp activity has led to attempts to inhibit P-gp activity in tumors of patients to improve their response to chemotherapy (5–8). One potential complication in this approach is the unknown effect that P-gp inhibitors may have due to inhibition of the natural function(s) of the endogenous P-gp present in many normal cells and tissues. To elucidate these natural functions, and to predict possible adverse effects of the use of P-gp blockers, we have generated mice with a genetic deficiency in one or more of their P-gp genes.

Whereas humans have only one P-gp conferring multidrug resistance (MDR1), mice have two, mdr1a (also called mdr3) and mdr1b (also called mdr1) (9–12), together probably fulfilling the same function(s) as the single human MDR1 P-gp. Mouse *mdr1a* is highly expressed in the intestinal epithelium and at the blood–brain and blood–testis barriers, whereas *mdr1b* is highly expressed in the adrenal gland, pregnant uterus, and ovaries. In addition, both genes are substantially expressed in many other tissues, including liver, kidney, lung, heart, and spleen (13, 14). The human MDR1 P-gp is present in the same tissues, and it was found to localize to the apical (excretory) membranes in intestine, liver, and kidney (15, 16).

Our previous analysis of mice with a deficiency in the *mdr1a* gene has established an important pharmacological role of the mdr1a P-gp in the blood–brain barrier, protecting the brain against entry of a range of toxic xenobiotics and drugs, and in the intestine, where it limits the entry of these compounds from the intestinal lumen, and even takes part in their active excretion from the bloodstream (14, 17–20). Disruption of the gene for the mdr2 P-gp, which is closely related to the mdr1a and mdr1b P-gps, showed that this protein is essential for phospholipid excretion in the liver (21).

The spectrum of compounds transported by the mdr1-type P-gps is enormous, and it includes, among others, endogenous corticosteroids like cortisol, corticosterone, and aldosterone (22). As a consequence, the range of additional physiological functions speculatively proposed for the mdr1-type P-gps is large, including among others the possibility that the high level of mdr1b P-gp in adrenal gland and pregnant uterus might be important for corticosteroid handling (21). To further investigate the physiological and pharmacological functions of the mdr1-type P-gps, we have generated and characterized mice with a deficiency in the *mdr1b* gene, and in both the *mdr1a* and *mdr1b* genes.

MATERIALS AND METHODS

Targeting of the *mdr1b* Gene and Generation of Knockout Mice. *mdr1b* genomic sequences were cloned from a mouse strain 129-derived CCE embryonic stem (ES) cell library. The backbone of the *mdr1b* targeting vector was a 9.6-kb *Apa*I fragment containing exons 3, 4, and 5 (Fig. 1*A*). Two small adjacent *Nco*I fragments together containing exons 3 and 4 were deleted and replaced by a *pgk-neo* cassette (14, 23). The resulting 10.8-kb *Apa*I–*Apa*I targeting fragment was electroporated into strain 129/Ola-derived E14 ES cells, and colonies resistant to 200 μg of G418 (GIBCO) per ml were isolated. Correct homologous recombination was checked by Southern

The publication costs of this article were defrayed in part by page charge payment. This article must therefore be hereby marked "*advertisement*" in accordance with 18 U.S.C. §1734 solely to indicate this fact.

0027-8424/97/944028-6$2.00/0
PNAS is available online at **http://www.pnas.org**.

Abbreviations: P-gp, P-glycoprotein; ES, embryonic stem; NK, natural killer.

‖To whom reprint requests should be addressed.

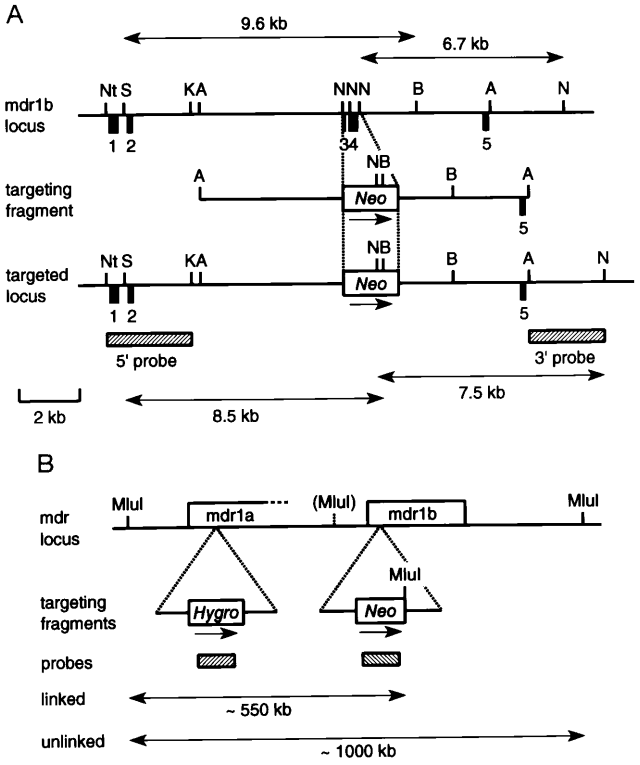

FIG. 1. Targeted disruption of the *mdr1b* gene. (*A*) Structure of part of the *mdr1b* gene, the *mdr1b* targeting fragment, and the targeted locus. Numbered black boxes represent exons. Transcriptional direction of the *neo* cassette is indicated. Hatched boxes, 5′ and 3′ probes. Double-headed arrows, position and size of restriction fragments diagnostic for the wild-type (*Upper*) and correctly targeted (*Lower*) locus. Restriction sites: Nt, *Not*I; S, *Sma*I; K, *Kpn*I; A, *Apa*I; N, *Nco*I; B, *Bam*HI. (Scale bar = 2 kb.) (*B*) Secondary targeting of the *mdr1b* locus (*neo* cassette) in a chromosome containing an *mdr1a* disruption (*hygro* cassette). Double-headed arrows indicate position and size of the *Mlu*I restriction fragments diagnostic for linked (≈550 kb) and unlinked (≈1000 kb) disruption of the *mdr1a* and *mdr1b* genes as detected with the *hygro* probe (left hatched box). Open boxes, genes and selectable cassettes. The 3′ end of the *mdr1a* gene is not yet mapped. (MluI) indicates a partially cut *Mlu*I site (likely due to partial CG methylation). Other designations are as in *A*.

blotting of *Sma*I/*Bam*HI or *Nco*I digests using a 2.8-kb *Not*I–*Kpn*I 5′ probe and a 2.4-kb *Apa*I–*Nco*I 3′probe, respectively. Absence of additional randomly integrated *pgk-neo* sequences was checked with a *neo* probe.

For secondary targeting in the *mdr1a* (+/−) ES cell clone 29 (14), the *mdr1b* targeting vector was modified by insertion of a symmetric *Xba*I–*Mlu*I–*Nru*I–*Mlu*I–*Xba*I linker (sequence: 5′-CTAGACGCGTCGCGACGCGT-3′) into an *Xba*I site directly 3′ of the *pgk-neo* cassette (Fig. 1*B*). Electroporation, selection, and screening for correct targeting of the *mdr1b* locus were as described above. Disruption of the *mdr1b* locus in the chromosome already containing the *mdr1a* disruption was verified by blotting *Mlu*I-digested genomic DNA, size separated in a CHEF system, onto filters, and subsequent probing with a *hygro* probe (Fig. 1*B*).

Chimeric mice were generated from ES clones by injection into C57/BL6 blastocysts and reimplantation as described before (14, 23). Genetic transmission of the disrupted alleles was checked by Southern blot or PCR analysis of isolated tail DNA. Our subsequent analyses were done on mice (10–14 weeks old unless noted otherwise) with a mixed genetic background (effectively F_3, F_4, and F_5 of a 129/Ola and FVB backcross) or FVB background (paclitaxel excretion experiment only).

Histology, Clinical Chemistry, Hematology. These routine analyses were carried out as described (14, 23). Serum levels of bilirubin, alkaline phosphatase, aspartate aminotransferase, alanine aminotransferase, lactate dehydrogenase, creatinine, urea, Na^+, K^+, Ca^{2+}, Cl^-, phosphate, total protein, and albumin were determined in male and female mice. Hemoglobin level, hematocrit, and erythrocyte, leucocyte, and thrombocyte counts were determined in heparinized blood.

Protein Analysis. Immunoblot analysis of P-gp content in tissue membrane fractions using monoclonal antibody C219 (Centocor) and visualization with the enhanced chemiluminescence method (Amersham) was carried out as described (14).

RNA Analysis. RNase protection procedures and the mouse *mdr1a*, *mdr1b*, *mdr2*, and *gapdh* probes were described before (14, 23). The mouse *mrp* and *oct-1* RNase protection probes will be described in detail elsewhere. The mouse *cftr* probe (a gift of B. J. Scholte, Erasmus University, Rotterdam, The Netherlands) covers exons 8–10 and yields a 425 nt protected fragment. *mdr2* expression was tested in liver, spleen, kidney, jejunum, heart, and lung; *mrp* expression in lung, liver, kidney, uterus, colon, and jejunum; *cftr* expression in lung, jejunum, colon, and liver; and *oct-1* expression in liver, kidney, uterus, jejunum, and colon. Mouse *spgp* RNA was detected on total liver RNA blots by cross-hybridization with a 1.6 kb partial cDNA clone (a47) encoding the amino-terminal ATP-binding site, linker region, and carboxyl-terminal transmembrane region of rat *spgp* (24).

Natural Killer (NK) Cell Activity–Cell Surface Phenotyping. Mice were injected i.p. with 100 μg poly(IC) (Sigma) 24 hr before harvesting the spleen to stimulate NK cell activity (25). Cytotoxic activity of spleen cells against the NK sensitive target cell YAC was measured with a standard ^{51}Cr release assay in Iscoves medium (GIBCO) supplemented with 10% fetal calf serum (BioWhittaker). Percentage specific lysis was measured as described (26).

Cell surface phenotyping of spleen cells, thymocytes, and lymph node cells of four male *mdr1a/1b* (−/−) and four male wild-type mice was performed by direct immunofluorescence with fluorescein isothiocyanate- and phycoerythrin-labeled monoclonal antibodies against CD4, CD8, CD11b (Mac-1), CD45, CD90.2 (Thy-1.2), and B220, all purchased from PharMingen. Cells were analyzed on a FACScan (Becton Dickinson).

Pharmacokinetic Analyses. Procedures for the pharmacokinetic analyses of [^{3}H]digoxin and paclitaxel in mice were as described (17, 19, 27). Drugs were injected into the tail vein. In gallbladder cannulation experiments, mice were anesthetized, the abdominal cavity was opened, and the common bile duct was ligated. The gallbladder was then cannulated and bile was collected over a 90-min time period after i.v. injection of the drug. At the end of the 90-min period, intestinal contents, plasma, liver, and brain were also collected, and levels of radioactivity and/or drugs were measured. [^{3}H]digoxin was measured by liquid scintillation counting and an immunoassay (TDxFLx, Abbott) detecting digoxin and its pharmacodynamically active metabolites, and paclitaxel by a sensitive and selective HPLC method. To avoid the moderate variation in absolute tissue concentrations sometimes observed when experiments were carried out far apart in time (>3 months), we only directly compared data from mice analyzed within a few days. Statistical significance of differences was assessed using Student's unpaired two-tailed *t*-test.

Rhodamine 123 Efflux from Bone Marrow Cells. Femoral bone marrow cells were partially purified by density gradient centrifugation followed by fluorescence-activated sorting of cells positive for binding of wheat germ agglutinin (WGA), and negative for binding of the myelomonocytic marker antibody 15–1.1 (28). These $WGA^+/15–1.1^-$ cells were stained with rhodamine 123 (0.1 μg/ml) for 20 min at 37°C, washed twice

at room temperature, and the subsequent efflux of rhodamine at 37°C was measured as described (28).

RESULTS

Generation and Characterization of *mdr1b* (−/−) Mice. The *mdr1b* gene was inactivated by homologous recombination in ES cells as outlined in Fig. 1*A*. Exons 3 and 4 in the 5′ part of the gene, encoding the first putative transmembrane segment of mdr1b P-gp and some flanking sequences, were deleted. In addition, this deletion results in a frame shift. We generated homozygous *mdr1b* (−/−) mice from two independently targeted ES clones. No full-length mdr1b P-gp was detectable anymore in immunoblots of adrenal gland membranes of *mdr1b* (−/−) mice. Despite the very high *mdr1b* expression normally found in the adrenal gland and in the pregnant uterus of wild-type mice (13, 29), *mdr1b* (−/−) mice displayed normal viability, fertility, and lifespan, and no obvious spontaneous physiological abnormalities were observed. We previously found that in *mdr1a* (−/−) mice the expression of *mdr1b* was increased in liver and kidney, suggesting possible compensatory expression between these functionally related genes. However, *mdr1a* expression was not significantly altered in any major organ of *mdr1b* (−/−) mice, as measured by RNase protection. The tissues tested included adrenal gland, uterus, liver, kidney, heart, lung, skeletal muscle, stomach, jejunum, cecum, colon, spleen, thymus, testis, ovary, uterus, and brain (results not shown). Extensive macroscopic and microscopic histological examination of all major organs did not reveal any abnormalities. Size and appearance of the adrenal gland were not unusual in *mdr1b* (−/−) mice.

The very high level of mdr1b P-gp in the endometrium and placental trophoblasts of the pregnant uterus has led to speculation about a possible physiological role of the protein during pregnancy, or in protection of the fetus against toxins (e.g., see ref. 30), analogous to the role of mdr1a P-gp in the blood–brain barrier. However, pregnancy and litter size were normal in *mdr1b* (−/−) mice. Furthermore, a pharmacokinetic analysis of the P-gp substrate drug [^{3}H]digoxin in approximately 17-day pregnant mice revealed no increase in [^{3}H]digoxin levels in *mdr1b* (−/−) fetuses of *mdr1b* (−/−) mothers, compared with wild-type fetuses of wild-type mothers (Table 1). This is not due to the inability of the mdr1b P-gp to transport digoxin: We have demonstrated that the mouse mdr1b P-gp can efficiently transport [^{3}H]digoxin (and [^{3}H]paclitaxel, see below) using *mdr1b*-transfected polarized LLC-PK1 pig kidney cells (results not shown). Table 1 also illustrates the very limited effect of the absence of the mdr1b P-gp on the overall pharmacokinetics of [^{3}H]digoxin. This contrasts sharply with the pronounced effects of the absence of the mdr1a P-gp in *mdr1a* (−/−) mice (17). Additional analyses indicated a somewhat increased accumulation of [^{3}H]digoxin in adrenal glands of *mdr1b* (−/−) males (632 ± 154 vs. 320 ± 60 ng/g) and possibly in ovaries of nonpregnant *mdr1b* (−/−) females (708 ± 401 vs. 288 ± 63 ng/g), but not in any other tissue examined.

Table 1. Tissue levels of radioactivity in pregnant *mdr1b* (+/+) and (−/−) mice 4 hr after i.v. injection of [^{3}H]digoxin (1 mg/kg)

Tissue	*mdr1b* (+/+)	*mdr1b* (−/−)	Ratio (−/−):(+/+)
Brain	13.5 ± 2.4	18.7 ± 3.8	1.4
Muscle	397 ± 47	288 ± 24	0.7
Heart	235 ± 55	243 ± 18	1.0
Kidney	319 ± 77	361 ± 82	1.1
Liver	727 ± 263	766 ± 119	1.1
Lung	176 ± 56	175 ± 14	1.0
Spleen	118 ± 35	120 ± 15	1.0
Colon	604 ± 116	574 ±128	1.0
Uterus	318 ± 89	219 ± 60	0.7
Placenta	322 ± 108	258 ± 43	0.8
Fetuses	105 ± 8	109 ± 6	1.0
Plasma	689 ± 343	764 ± 81	1.1

Results are means ± SD in nanograms per gram tissue ([^{3}H]digoxin equivalent). Three pregnant mice were analyzed in each group. All fetuses of each mother were pooled.

Generation and Characterization of *mdr1a/1b* (−/−) Mice. The lack of biological effects of the *mdr1b* gene disruption might be explained by the abundant mdr1a P-gp taking over the physiological roles of the mdr1b P-gp. We therefore generated mice deficient for both the mdr1a and the mdr1b P-gps. The very close linkage of the *mdr1a* and *mdr1b* genes (31) made it virtually impossible to obtain these mice by conventional crossing of *mdr1a* (−/−) and *mdr1b* (−/−) mice, so we had to resort to the generation of ES cells with a linked disruption of both the *mdr1a* and *mdr1b* genes. This was achieved by a secondary targeting of the *mdr1b* gene in a pluripotent ES cell clone already containing a heterozygous disruption of the *mdr1a* gene. This clone (nr. 29) was previously used to generate one of our *mdr1a* (−/−) strains (14). An *Mlu*I linker inserted 3′ of the *neo* cassette allowed detection of *mdr1b* targeting linked to the *mdr1a* disruption (the *hygro* cassette) by long-range restriction mapping (see Fig. 1*B*). Although the total frequency of correct targeting of the *mdr1b* gene was lower in this case than in the original targeting of the *mdr1b* gene in E14 ES cells (about 2% vs. originally 25%), both *mdr1b* alleles were targeted with comparable efficiency: 5 of 11 correctly targeted clones had inserted the *neo* cassette adjacent to the disrupted *mdr1a* gene (data not shown).

We succeeded in generating homozygous *mdr1a/1b* (−/−) mice from two independently targeted ES clones, demonstrating the feasibility of generating mice with disruptions of closely linked genetic loci by sequential gene targeting in ES cells. Immunoblot analysis of adrenal gland membranes proved that no mdr1b (or mdr1a) P-gp was detectable anymore in *mdr1a/1b* (−/−) mice (Fig. 2).

Remarkably, *mdr1a/1b* (−/−) mice displayed completely normal development, viability, and fertility (currently analyzed up to 1 year of age). Macroscopic and microscopic examination of all major organs did not reveal any clear abnormalities, nor did an extensive analysis of serum clinical chemistry and hematological parameters (see *Materials and Methods*). We observed no systematic differences in body weight. Bile flow and biliary output of phospholipids, bile acids, cholesterol, and glutathione were normal (R. P. J. Oude Elferink, personal communication).

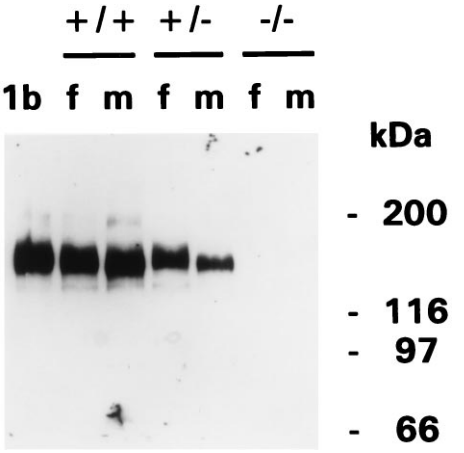

FIG. 2. Absence of P-gp in adrenal glands of *mdr1a/1b* (−/−) mice. Protein immunoblot analysis of adrenal gland membrane fractions (10 μg per lane) using monoclonal antibody C219. *mdr1a/1b* genotypes and protein marker sizes are indicated. f, female; m, male. Lane 1b contains a membrane fraction isolated from *mdr1b*-transfected SW1573 (lung cancer) cells.

The MDR1 P-gp level is relatively high in human CD56$^+$ NK cells (32, 33), and based on inhibition studies with reversal agents it has been suggested that P-gps might be involved in NK cell-mediated cytotoxicity (34). However, we found no difference in NK cell activity between *mdr1a/1b* (−/−) or wild-type splenocytes using NK-sensitive YAC-1 tumor cells as target in a chromium release cytotoxicity assay (data not shown). We also tested a range of immunohematological parameters, including absolute and relative numbers of CD4- and CD8-positive or -negative thymocytes, splenocytes, and lymph node cells, the presence of Mac-1$^+$ cells, and the relative amounts of CD4/CD45-positive or -negative cells. Furthermore, the relative abundance of Thy-1/B220-positive or -negative cells was tested in the spleen. Again, no systematic differences were observed, suggesting that *mdr1a/1b* (−/−) mice have no gross abnormalities in development or differentiation of the lymphocyte compartment, in spite of the widespread differential presence of P-gp here (32, 33, 35–37).

Considering the variety of speculative physiological functions attributed to the mdr1-type P-gps, one could envisage that several other functionally or structurally related genes might compensate for the absence of the P-gps in *mdr1a/1b* (−/−) mice through up-regulation of the expression in affected tissues. Using RNase protection, we have checked for alterations in expression of the mouse *mdr2*, *mrp*, *cftr*, and *oct-1* (38) genes in a range of tissues of wild-type and *mdr1a/1b* (−/−) mice. Expression of the mouse sister of P-gp (*spgp*) gene (24) in liver was tested using total RNA blots. We found no altered expression of any of these genes (data no shown).

Pharmacokinetic Alterations in *mdr1a/1b* (−/−) Mice. Because the *mdr1a/1b* (−/−) mice appeared to be physiologically normal overall, we next tested for changes in pharmacokinetics using the drug [^{3}H]digoxin, previously found to be a useful probe for this purpose (17, 19). The tissue distribution of [^{3}H]digoxin in *mdr1a/1b* (−/−) mice was very similar to that in *mdr1a* (−/−) mice (17), demonstrating the same marked increase in brain and (in males, not shown) testis accumulation and similarly increased plasma levels compared with wild-type mice 4 hr after i.v. injection of 1 mg/kg (Table 2). In addition, [^{3}H]digoxin accumulation in adrenal gland and ovaries was increased significantly more than the plasma levels, and than the levels in most other tissues tested. This supports the results found in *mdr1b* (−/−) mice, and suggests that the very high levels of mdr1b P-gp normally present in a substantial fraction of the cells in these two tissues can decrease the overall accumulation of drugs or other compounds transported by P-gp.

Table 2. Tissue levels of radioactivity in female *mdr1a/1b* (+/+) and (−/−) mice 4 hr after i.v. injection of [^{3}H]digoxin (1 mg/kg)

Tissue	*mdr1a/1b* (+/+)	*mdr1a/1b* (−/−)	Ratio (−/−):(+/+)
Brain	37.1 ± 5.6	1,011 ± 162	27.2**
Muscle	329 ± 26	606 ± 134	1.8
Heart	245 ± 36	645 ± 98	2.6
Kidney	303 ± 30	774 ± 141	2.6
Liver	857 ± 116	2,180 ± 186	2.5
Lung	229 ± 10	603 ± 61	2.6
Spleen	131 ± 28	347 ± 61	2.6
Thymus	286 ± 65	792 ±134	2.8
Lymph nodes	167 ± 36	663 ± 158	3.9
Adrenal gland	500 ± 17	3,076 ± 979	6.2*
Uterus	170 ± 13	379 ± 65	2.2
Ovary	545 ± 105	4,190 ± 474	7.7**
Plasma	622 ± 73	1,775 ± 318	2.9

Results are means ± SD in nanograms per gram tissue ([^{3}H]digoxin equivalent). Three mice were analyzed in each group. Asterisks: significantly increased in *mdr1a/1b* (−/−) mice after normalization for the increased plasma levels. *$P < 0.05$; **$P < 0.002$.

The elimination rate of [^{3}H]digoxin from plasma of *mdr1a/1b* (−/−) mice appeared to be only slightly reduced compared with that in *mdr1a* (−/−) mice (data not shown). This was surprising, because we had expected that the increased levels of mdr1b P-gp in liver and kidney of *mdr1a* (−/−) mice (14) might substantially contribute to the excretion of this compound. In that case, the removal of mdr1b P-gp in *mdr1a/1b* (−/−) mice should lead to a marked decrease in liver-mediated digoxin excretion. Direct measurement of this excretion after cannulation of the gallbladder, and ligation of the common bile duct to prevent biliary flux into the intestine, showed only a moderate (albeit significant) decrease relative to wild-type mice (Table 3). Compared with *mdr1a* (−/−) mice, biliary [^{3}H]digoxin excretion was not decreased (compare with ref. 19). An immunoassay demonstrated that more than 95% of the radioactivity excreted in bile of wild-type and *mdr1a/1b* (−/−) mice represented digoxin and closely related, pharmacologically active metabolites. This result shows that the liver harbors a substantial [^{3}H]digoxin excretion capacity that is distinct from the mdr1-type P-gps. In contrast, the direct intestinal excretion in *mdr1a/1b* (−/−) mice was sharply decreased (Table 3), similar to what we previously found in *mdr1a* (−/−) mice (19). The urinary excretion of [^{3}H]digoxin was not impaired in *mdr1a/1b* (−/−) mice, indicating that mdr1-type P-gps are not essential for digoxin excretion by the kidney (not shown). Thus, the limited effect of the mdr1b P-gp by itself on the plasma pharmacokinetics of digoxin appears to result from the presence of effective alternative digoxin excretion mechanisms in both liver and kidney, and from the fact that *mdr1b* is not expressed in the intestinal epithelium. In contrast, the predominant role of the mdr1a P-gp in the plasma pharmacokinetics of digoxin appears to result mainly from its high intestinal expression (19, 20).

In a comparable gallbladder cannulation experiment, we found that the biliary excretion of the anticancer drug paclitaxel (Taxol) was not significantly decreased in *mdr1a/1b* (−/−) mice compared with wild-type mice (5.2 ± 2.9% vs. 5.9 ± 3.4%), whereas the intestinal excretion dropped markedly (Table 4). These results demonstrate that, apart from the mdr1a and mdr1b P-gps, there must be at least one other efficient transporter for paclitaxel (and for digoxin) in the liver of mice. In view of the potential contribution of this transporter to the development of drug resistance against this important anticancer drug, its identification should have a high priority.

P-gp Activity in Bone Marrow. Substantial P-gp levels have been found in hematopoietic stem cells, and in several more differentiated hematological subclasses (32, 33, 35, 36, 39). In fact, an important tool in the isolation of pluripotent hematopoietic stem cells (conferring both short-term and long-term bone marrow repopulation) is the differential capacity of these cells to extrude the synthetic dye rhodamine 123, a well-established substrate of the mdr1-type P-gps. It has therefore

Table 3. Biliary and intestinal excretion of [^{3}H]digoxin-derived radioactivity in *mdr1a/1b* (+/+) and *mdr1a/1b* (−/−) mice with a cannulated gallbladder

	mdr1a/1b (+/+)	*mdr1a/1b* (−/−)
Biliary excretion (% of dose)	21.0 ± 3.4	13.6 ± 4.1*
Intestinal excretion (% of dose)	16.1 ± 2.9	1.5 ± 0.3**
Plasma level (ng/ml) at 90 min	21.2 ± 3.8	39.6 ± 5.1**

Female mice with a cannulated gallbladder and ligated common bile duct received an i.v. injection of [^{3}H]digoxin (0.05 mg/kg). Bile was collected for 90 min. Intestinal contents and plasma levels were measured at the end of this period. Results are means ± SD ($n = 4$). *$P < 0.05$; **$P < 0.002$.

Table 4. Biliary and intestinal excretion of paclitaxel in *mdr1a/1b* (+/+) and *mdr1a/1b* (−/−) mice with a cannulated gallbladder

	mdr1a/1b (+/+)	*mdr1a/1b* (−/−)
Biliary excretion (% of dose)	5.9 ± 3.4	5.2 ± 2.9
Intestinal excretion (% of dose)	3.5 ± 0.8	0.8 ± 0.4**
Plasma level (ng/ml) at 90 min	289 ± 76	313 ± 77

Female mice with a cannulated gallbladder and ligated common bile duct received an i.v. injection of paclitaxel (5 mg/kg). Bile was collected for 90 min. Intestinal contents and plasma levels were measured at the end of this period. Results are means ± SD ($n = 4$). **$P < 0.002$.

been proposed that mdr1-type P-gps could be a major factor responsible for the low accumulation of rhodamine 123 and other dyes in these cells (refs. 28 and 40 and references therein, ref. 41). To test this hypothesis, we measured the rate of rhodamine 123 efflux from partially purified hematopoietic progenitor cells isolated from wild-type, *mdr1a* (−/−), *mdr1b* (−/−), and *mdr1a/1b* (−/−) bone marrow. Fig. 3 shows that the rate of rhodamine efflux was diminished in *mdr1a* (−/−) and in *mdr1b* (−/−) cells relative to wild-type, whereas this rate was strongly decreased in *mdr1a/1b* (−/−) cells. Wild-type granulocytes, which do not have substantial rhodamine efflux capacity (32, 33), were included as a negative control. These results prove that the mdr1-type P-gps are the main determinant of low rhodamine accumulation in hematopoietic progenitor cells, and they show that both mdr1a and mdr1b P-gp make a substantial functional contribution to drug extrusion from this compartment.

DISCUSSION

The most significant outcome of this study is the lack of biological effects of the removal of mdr1-type P-gps from mice. In spite of the huge range of physiological and nonphysiological, natural and (semi-)synthetic substrates that can be transported by these proteins, and in spite of the high levels of these proteins in a range of vital organs, *mdr1a/1b* (−/−) mice live and breed quite normally, at least under laboratory conditions. The only phenotype(s) observed so far relates to the contribution of the mdr1a and mdr1b P-gps to the tissue distribution, cellular accumulation, and excretion of a range of transported drugs.

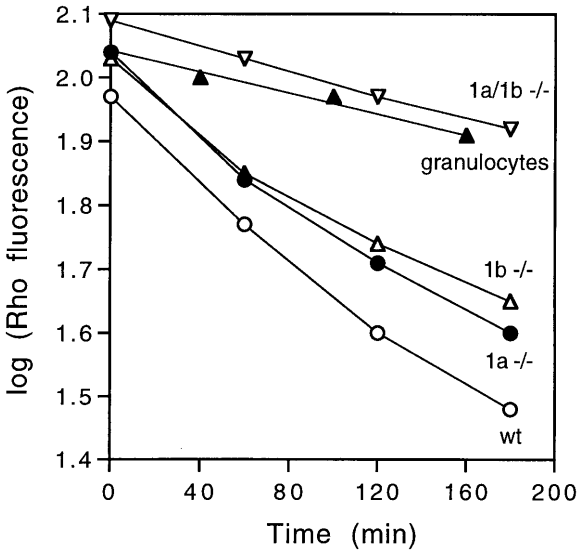

FIG. 3. Rhodamine efflux from wild-type, *mdr1a* (−/−), *mdr1b* (−/−), and *mdr1a/1b* (−/−) bone marrow cells. Partially purified ($WGA^+/15–1.1^-$) bone marrow progenitor cells were loaded with rhodamine 123. Subsequent efflux in rhodamine-free medium was measured by fluorescence-activated cell sorting. Qualitatively comparable results were obtained in three out of three independent experiments. (○), wild-type cells; (●), *mdr1a* (−/−) cells; (△), *mdr1b* (−/−) cells; (▽), *mdr1a/1b* (−/−) cells; (▲), wild-type granulocytes.

The list of physiological functions speculatively attributed to the mdr1-type P-gps is long (e.g., see ref. 21). Although our analysis of possible functional abnormalities has not been exhaustive it nevertheless shows that the mdr1-type P-gps are not vital to basic liver, kidney, or intestinal function, nor to the functions of the brain, adrenal gland, ovaries, or uterus during pregnancy. The same holds true for the hematopoietic stem cells and the hematological compartment in general. Basic deficiencies in the functioning of any of these tissues should have resulted in abnormalities that would have shown up in our analyses. Nevertheless, we are still continuing a search for more subtle abnormalities in *mdr1a/1b* (−/−) mice. The recent availability of *mdr1a/1b* (−/−) mice in a homogeneous, well-breeding genetic background (by systematic backcrossing to the FVB strain) will facilitate such a search as it limits the background variability in the parameters studied owing to genetic variation. Our current analysis was mainly done in a mixed genetic background.

The lack of an observable biological phenotype in *mdr1a/1b* (−/−) mice may mean that for many of the proposed biological functions other protein systems exist that can take over. It may also simply mean that mdr1-type P-gps play no significant role in these physiological functions, and that their main, if not exclusive, role is in the protection of the organism against naturally occurring toxins. A limited survey of other genes that might take over in the absence of P-gps yielded no changes in RNA levels, but we cannot exclude changes in other untested or as yet unknown genes.

An important implication of our study is that it may be acceptable to completely block MDR1 P-gp activity in humans at least transiently without affecting vital biological functions. This could have consequences for several pharmacological applications using inhibitors of MDR1 P-gp, such as the use of reversal agents to selectively increase the penetration of antitumor drugs in multidrug resistant tumor cells. Perhaps more readily attainable might be the use of P-gp inhibitors to increase the oral bioavailability of drugs that are largely excluded and extruded from the body by the intestinal P-gp activity, and to extend the plasma half-life of drugs when this is desirable for therapeutic or economic reasons. It may even be feasible to increase the passage of certain drugs across the blood–brain barrier, which might profoundly extend the range of drugs available for treatment of central nervous system disorders.

Several caveats should be added, however: first, humans may not be as impervious to the absence of mdr1-type P-gp activity as mice. Second, the continuous absence of mdr1-type P-gps during development may have resulted in essential adaptations in *mdr1a/1b* (−/−) mice that cannot readily be deployed upon acute pharmacological blocking of P-gp. Third, the reversal agent used should be highly specific for the MDR1 P-gp to prevent unpredictable side effects due to blocking of other protein systems. Nevertheless, our results indicate that it is worthwhile to further pursue the development of more effective and specific P-gp inhibitors. Ultimately, the safety and feasibility of their use in humans can only be assessed in clinical studies.

In expectation of this, we think that *mdr1a/1b* knockout mice provide a useful model system that will help to establish the principal contributions of the mdr1-type P-gps to the pharmacokinetics of drugs of interest. Moreover, by comparing the pharmacokinetics of drugs in *mdr1a/1b* (−/−) and wild-type mice in the presence or absence of P-gp reversal

agents, one can assess both the effectivity and the specificity of these reversal agents. Thus, these mice can help in the search for more sophisticated reversal agents. Also, the absence of the mdr1-type P-gps in *mdr1a/1b* (−/−) mice makes it easier to study other transport systems that share substrates with the mdr1-type P-gps. This is clearly illustrated by our finding of substantial [^{3}H]digoxin and paclitaxel excretion activity in the liver of *mdr1a/1b* (−/−) mice. We are currently pursuing these pharmacological questions.

Our rhodamine efflux results provide direct proof that endogenous P-gp in hematopoietic progenitor cells can contribute to the decreased accumulation of substrate drugs in these cells. One important implication of this finding is that systemic reversal strategies successful in inhibiting P-gp in drug-resistant malignant cells, thus increasing their sensitivity to cytotoxic drugs, may likewise increase the sensitivity of susceptible hematopoietic progenitor cells. Since bone marrow toxicity is often dose-limiting in cancer chemotherapy regimens, this may present a serious hurdle to the successful application of reversal agents in cancer chemotherapy.

We thank Dr. A. J. M. Berns for crucial support, Drs. V. Ling and S. Childs (Vancouver) for the rat *spgp* probe, Dr. B. J. Scholte (Rotterdam, The Netherlands) for the mouse *cftr* probe, R. Bobeldijk and C. Brouwers for performing expert blastocyst injections, Dr. J. H. Beijnen for digoxin immunoassays, and A. J. Schrauwers for excellent biotechnical assistance. U.M. is a fellow of the European Cancer Center. This work was supported in part by Grant NKI 92-41 of the Dutch Cancer Society to P.B.

1. Endicott, J. A. & Ling, V. (1989) *Annu. Rev. Biochem.* **58,** 137–171.
2. Roninson, I. B. (1992) *Biochem. Pharmacol.* **43,** 95–102.
3. Ruetz, S. & Gros, P. (1994) *Trends Pharmacol. Sci.* **15,** 260–263.
4. Gottesman, M. M., Hrycyna, C. A., Schoenlein, P. V., Germann, U. A. & Pastan, I. (1995) *Annu. Rev. Genet.* **29,** 607–649.
5. Tsuruo, T., Iida, H., Tsukagoshi, S. & Sakurai, Y. (1981) *Cancer Res.* **41,** 1967–1972.
6. Dalton, W. S., Grogan, T. M., Meltzer, P. S., Scheper, R. J., Durie, B. G. M., Taylor, C. W., Miller, T. P. & Salmon, S. E. (1989) *J. Clin. Oncol.* **7,** 415–424.
7. Ford, J. M. & Hait, W. N. (1990) *Pharmacol. Rev.* **42,** 155–199.
8. Sikic, B. I. (1993) *J. Clin. Oncol.* **11,** 1629–1635.
9. Chen, C. J., Chin, J. E., Ueda, K., Pastan, I., Gottesman, M. M. & Roninson, I. B. (1986) *Cell* **47,** 381–389.
10. Gros, P., Croop, J. & Housman, D. (1986) *Cell* **47,** 371–380.
11. Hsu, S. I.-H., Lothstein, L. & Horwitz, S. B. (1989) *J. Biol. Chem.* **264,** 12053–12062.
12. Devault, A. & Gros, P. (1990) *Mol. Cell. Biol.* **10,** 1652–1663.
13. Croop, J. M., Raymond, M., Haber, D., Arceci, R. J., Gros, P. & Housman, D. E. (1989) *Mol. Cell. Biol.* **9,** 1346–1350.
14. Schinkel, A. H., Smit, J. J. M., van Tellingen, O., Beijnen, J. H., Wagenaar, E., van Deemter, L., Mol, C. A. A. M., van der Valk, M. A., Robanus-Maandag, E. C., te Riele, H. P. J., Berns, A. J. M. & Borst, P. (1994) *Cell* **77,** 491–502.
15. Thiebaut, F., Tsuruo, T., Hamada, H., Gottesman, M. M., Pastan, I. & Willingham, M. C. (1987) *Proc. Natl. Acad. Sci. USA* **84,** 7735–7738.
16. Cordon-Cardo, C., O'Brien, J. P., Casals, D., Ritmann-Grauer, L., Biedler, J. L., Melamed, M. R. & Bertino, J. R. (1989) *Proc. Natl. Acad. Sci. USA* **86,** 695–698.
17. Schinkel, A. H., Wagenaar, E., van Deemter, L., Mol, C. A. A. M. & Borst, P. (1995) *J. Clin. Invest.* **96,** 1698–1705.
18. Schinkel, A. H., Wagenaar, E., Mol, C. A. A. M. & van Deemter, L. (1996) *J. Clin. Invest.* **97,** 2517–2524.
19. Mayer, U., Wagenaar, E., Beijnen, J. H., Smit, J. W., Meijer, D. K. F., van Asperen, J., Borst, P. & Schinkel, A. H. (1996) *Br. J. Pharmacol.* **119,** 1038–1044.
20. Sparreboom, A., van Asperen, J., Mayer, U., Schinkel, A. H., Smit, J. W., Meijer, D. K. F., Borst, P., Nooijen, W. J., Beijnen, J. H. & van Tellingen, O. (1997) *Proc. Natl. Acad. Sci. USA* **94,** 2031–2035.
21. Borst, P. & Schinkel, A. H. (1996) *Eur. J. Cancer* **32,** 985–990.
22. Ueda, K., Okamura, N., Hirai, M., Tanigawara, Y., Saeki, T., Kioka, N., Komano, T. & Hori, R. (1992) *J. Biol. Chem.* **267,** 24248–24252.
23. Smit, J. J. M., Schinkel, A. H., Oude Elferink, R. P. J., Groen, A. K., Wagenaar, E., van Deemter, L., Mol, C. A. A. M., Ottenhoff, R., van der Lugt, N. M. T., van Roon, M. A., van der Valk, M. A., Offerhaus, G. J. A., Berns, A. M. & Borst, P. (1993) *Cell* **75,** 451–462.
24. Childs, S., Lin Yeh, R., Georges, E. & Ling, V. (1995) *Cancer Res.* **55,** 2029–2034.
25. Lattime, E. C., Pecoraro, G. A. & Stutman, O. (1983) *J. Exp. Med.* **157,** 1070–1085.
26. Spits, H., IJssel, H., Terhorst, C. & de Vries, J. E. (1982) *J. Immunol.* **128,** 95–99.
27. Sparreboom, A., van Tellingen, O., Nooijen, W. J. & Beijnen, J. H. (1996) *Cancer Res.* **56,** 2112–2115.
28. Zijlmans, J. M. J. M., Visser, J. W. M., Kleiverda, K., Kluin, P. M., Willemze, R. & Fibbe, W. E. (1995) *Proc. Natl. Acad. Sci. USA* **92,** 8901–8905.
29. Arceci, R. J., Croop, J. M., Horwitz, S. B. & Housman, D. E. (1988) *Proc. Natl. Acad. Sci. USA* **85,** 4350–4354.
30. Gottesman, M. M. (1993) *Cancer Res.* **53,** 747–754.
31. Raymond, M., Rose, E., Housman, D. E. & Gros, P. (1990) *Mol. Cell. Biol.* **10,** 1642–1651.
32. Drach, D., Zhao, S., Drach, J., Mahavedia, R., Gattringer, C., Huber, H. & Andreeff, M. (1992) *Blood* **80,** 2729–2734.
33. Klimecki, W. T., Futscher, B. W., Grogan, T. M. & Dalton, W. S. (1994) *Blood* **83,** 2451–2458.
34. Chong, A. S.-F., Markham, P. N., Gebel, H. M., Bines, S. D. & Coon, J. S. (1993) *Cancer Immunol. Immunother.* **36,** 133–139.
35. Witkowski, J. M., Li, S. P., Gorgas, G. & Miller, R. A. (1994) *J. Immunol.* **153,** 658–665.
36. Bommhardt, U., Cerotinni, J.-C. & MacDonald, H. R. (1994) *Eur. J. Immunol.* **24,** 2974–2981.
37. Gupta, S. & Aggarwal, S. (1996) *Immunologist* **4,** 86–90.
38. Gründemann, D., Gorboulev, V., Gambaryan, S., Veyhl, M. & Koepsell, H. (1994) *Nature (London)* **372,** 549–552.
39. Chaudhary, P. & Roninson, I. B. (1991) *Cell* **66,** 85–94.
40. Li, C. L. & Johnson, G. R. (1992) *J. Exp. Med.* **175,** 1443–1447.
41. Goodell, M. A., Brose, K., Paradis, G., Conner, A. S. & Mulligan, R. C. (1996) *J. Exp. Med.* **183,** 1797–1806.